Tailoring the Permselectivity of Water Desalination Membranes via Nanoparticle Assembly

ARTICLE *in* LANGMUIR · JANUARY 2014

Impact Factor: 4.46 · DOI: 10.1021/la403718x · Source: PubMed

6 AUTHORS, INCLUDING:

Edwin P Chan
National Institute of Standards and Technolo…
39 PUBLICATIONS **1,040** CITATIONS
SEE PROFILE

Christopher M Stafford
National Institute of Standards and Technolo…
119 PUBLICATIONS **3,824** CITATIONS
SEE PROFILE

Langmuir

Article

pubs.acs.org/Langmuir

Tailoring the Permselectivity of Water Desalination Membranes via Nanoparticle Assembly

Edwin P. Chan,[†] William D. Mulhearn,[‡] Yun-Ru Huang,[‡] Jung-Hyun Lee,[§] Daeyeon Lee,*[,‡] and Christopher M. Stafford*[,†]

[†]Materials Science and Engineering Division, National Institute of Standards and Technology, 100 Bureau Drive, MS 8542, Gaithersburg, Maryland. 20899 United States

[‡]Department of Chemical and Biomolecular Engineering, University of Pennsylvania, 220 S. 33rd Street, Philadelphia, Pennsylvania. 19104 United States

[§]Center for Materials Architecturing, Korea Institute of Science and Technology (KIST), Seoul 136-791, Korea

Supporting Information

ABSTRACT: Thin film composite membranes can selectively separate mono- and divalent ions from water via solution-diffusion of each species through a dense but ultrathin, highly cross-linked polymer "skin" layer; water is transported across the membrane faster than associated salts. Changing the selectivity of the "skin" layer typically requires adjusting the monomer chemistries that make up the polymer "skin" layer, but doing so also impacts a host of other membrane properties. Here, we employ electrostatic layer-by-layer deposition of inorganic nanoparticles to enhance the permselectivity of an existing commercial nanofiltration membrane. We chose this approach because it is simple and robust and does not require any change to the underlying chemistry of the thin film composite (TFC) membrane. We found that a single layer of nanoparticles was sufficient to increase the permselectivity of the membrane by nearly 50%, compared to the virgin TFC membrane. In order to understand the mechanism for permselectivity enhancement, we developed a modified solution-diffusion model to account for the additional hydraulic resistance of the nanoparticle layer, which can faithfully capture the effect of nanoparticle layer thickness on the observed water and salt flux of the modified TFC membrane.

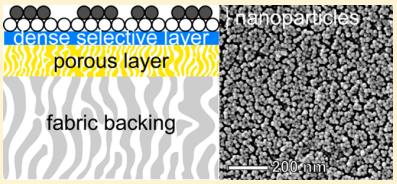

1. INTRODUCTION

The current state-of-the art water desalination technology is based on pressure-induced permeation of seawater through a polymer-based thin film composite (TFC) membrane.[1] Specific to desalination via reverse osmosis (RO), the TFC consists of three discrete polymer layers: (1) a dense polyamide selective layer that facilitates separation of salt from seawater based on differences in diffusion coefficients, (2) a porous polysulfone intermediate layer, and (3) a polyester fabric backing layer. Both the polysulfone and polyester layers are porous and designed for mechanical support; thus, the performance of the TFC membrane is primarily determined by the permselective properties of the polyamide selective layer. Since permselectivity of the polyamide layer, which is the ability to discriminate salt from water for an RO TFC membrane, is intimately linked with the polymer's network structure and chemistry, it is difficult to tune membrane performance without changing the monomer chemistry that is used to fabricate the selective layer.[2] For instance, a seemingly simple change in monomer chemistry directly impacts all aspects of the membrane, from the reactivity and kinetics of membrane formation to the network structure and dynamics of the resulting polyamide to the fouling propensity of the membrane surface.

One strategy to modify the performance of TFC membranes without resorting to fabricating an entirely new selective layer is via surface modification. Previously, surface modification has been applied to water desalination membranes to enhance salt rejection via deposition of *N*-isopropylacrylamide-*co*-acrylic acid copolymers onto the surface of a polyamide selective layer.[3] A similar strategy was used to improve resistance to chlorine degradation[4,5] and biofouling[6−9] by grafting organic molecules onto the selective layer surface. These demonstrations illustrate the versatility of surface modification in imparting functionality onto existing materials without the need for sophisticated chemistry, instrumentation, and long processing time, which is especially attractive for commercial water desalination membranes.

A very simple yet highly customizable class of surface modification is layer-by-layer (LbL) assembly of monomeric,[10−13] polymeric,[14−16] or inorganic materials.[17−20] In general, LbL assembly involves alternating deposition of at least two different reactive or oppositely charged species, which can include monomers, polyelectrolytes or nanoparticles, on the surface of interest to form a coating whose properties can be tuned by changing the assembly conditions such as pH, ionic strength and polyelectrolyte or nanoparticle sizes. In this work,

Received: September 26, 2013
Revised: December 17, 2013
Published: January 6, 2014

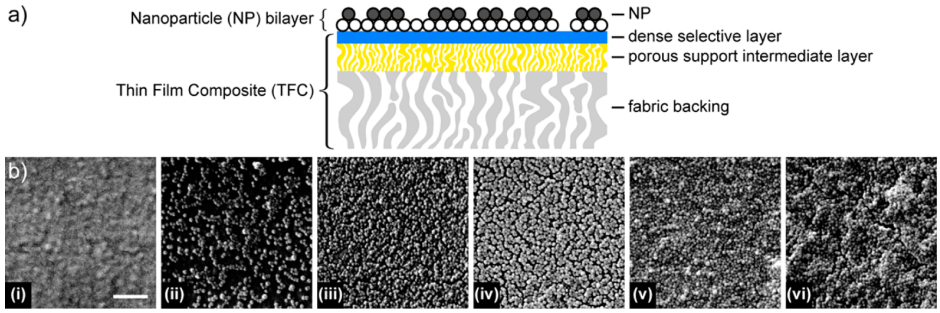

Figure 1. (a) Schematic of the nanoparticle-modified thin film composite (np-TFC) consisting of a single bilayer of nanoparticles assembled on the surface of the TFC membrane. (b) Top-down secondary electron micrographs of the (i) neat TFC membrane (TFC), (ii) 0.5 bilayer (np-TFC0.5+), (iii) 0.5 bilayer (np-TFC0.5-), (iv) 1 bilayer (np-TFC1), (v) 2 bilayer (np-TFC2), and (vi) 4 bilayer (np-TFC4). Scale bar for all micrographs is 200 nm.

we present a surface modification approach based on LbL assembly of charged colloidal nanoparticles, which have previously been shown to generate layers (on silicon substrates) with 35% to 50% porosity depending on choice of particle sizes and assembly conditions.[18,20,21] Charged nanoparticles provide a great deal of synthetic control since we can utilize LbL to alternatively deposit cationic and anionic nanoparticle (np) layers to fabricate nanoparticle-modified thin film composites (np-TFC) with tunable surface properties. We find that the presence of even a single layer of nanoparticles changes the performance of the commercial desalination membrane, i.e., reduced salt passage but an associated decrease in water flux. The mechanism of this performance change, which is quantified by modifying the traditional solution-diffusion model used to describe dense membranes, can be explained in terms of an enhancement in the hydraulic resistance due to the additional nanoparticle layer.

2. EXPERIMENTAL METHODS

General. Equipment and instruments or materials are identified in the manuscript in order to adequately specify the experimental details. Such identification does not imply recommendation by the National Institute of Standards and Technology, nor does it imply the materials are necessarily the best available for the purpose.

Nanoparticle Membrane Fabrication. Nanoparticle-modified membranes were fabricated on commercial TFC membranes via LbL nanoparticle assembly. The anionic particles were Ludox HS-30 colloidal silica with a nominal diameter of 12 nm. The cationic particles were Ludox CL-30 colloidal silica with a nominal diameter of 22 nm. Aqueous stock suspensions (30% by mass) of nanoparticles were obtained from Sigma Aldrich. The stock suspensions were diluted to a concentration of 0.03% by mass using deionized (DI) water, stirred thoroughly, and titrated to pH 3.0, which is known to give optimized nanoparticle LbL film growth, as previously reported.[19,20]

A commercial nanofiltration TFC membrane (Dow FILMTEC NF270) was used as the substrate for fabricating nanoparticle thin film composites (np-TFCs) via LbL assembly (Figure 1). Individual NF270 membranes were cut from a stock roll into 65 mm × 65 mm squares and soaked in DI water overnight prior to coating. The NF270 membrane was then secured to a silicon wafer support via a plastic frame, which facilitated handling of the membrane during deposition as well as ensured that the nanoparticles did not deposit on the backside of the membrane. It has been shown that the surface of NF270 membranes exhibits a net negative charge due to unreacted carboxylic acids; therefore, the np-TFCs were prepared by first soaking NF270 in the cationic nanoparticle suspension followed by soaking in the anionic nanoparticle solution. The membranes were immersed in the nanoparticle solutions for 10 min, followed by two rinses in DI water for 2 min each. These steps were repeated to create np-TFCs with 1, 2, and 4 bilayers (1 bilayer being defined as the deposition of one cationic and one anionic layer). We also prepared np-TFCs with just a single deposition of either the cationic or anionic nanoparticles; these membranes are thus designated as having 0.5 bilayer of particles. The fabricated np-TFCs are summarized in Table 1.

Table 1. Summary of np-TFCs Fabricated

sample name	NP bilayers x	"+" NP (Ludox CL-30) diameter, $2r_p$ (nm)	"−" NP (Ludox HS-30) diameter, $2r_p$ (nm)
np-TFC0.5+	0.5	22	
np-TFC0.5-	0.5		12
np-TFC1	1	22	12
np-TFC2	2	22	12
np-TFC4	4	22	12

Membrane Performance Testing. Membrane performance was tested against 150 mg/L NaCl aqueous solutions in a stirred dead-end filtration cell (Sterlitech HP4750). The active membrane area was 14.6 cm^2. Water flux and salt rejection were measured while operating at a pressure of 1.72 MPa (250 psi), and data points were taken at volume increments of ~14 mL. Water flux (J_w) was determined from the amount of permeate (V) divided by the membrane area (A) and time increment (t).

$$J_w = V/At \quad (1)$$

Salt rejection (R) was calculated from the salt concentration in the feed (C_f) and permeate (C_p), as determined by conductivity measurements (Orion 3 Star Plus, Thermo Scientific).

$$R(\%) = 100 \times (1 - C_p/C_f) \quad (2)$$

The average flux and rejection of a given membrane were taken from multiple aliquots over the first 45 min of testing, and the reported values are the average from at least three different membrane samples.

Membrane Morphology Characterization. Scanning electron microscopy (SEM) images were taken using a FEI-600 Quanta microscope. The sample surface was sputtered with a thin layer of iridium before imaging to prevent charging. The SEM images were captured at an accelerating voltage of 10 kV for virgin membranes, 15 kV for 1- and 2-bilayer nanoparticle-coated membranes, and 20 kV for 0.5- as well as 4-bilayer nanoparticle-coated membranes. The working distance was 10 mm.

3. RESULTS AND DISCUSSION

Figure 2 shows the water flux and salt rejection performance results for all of the membranes investigated. Generally, the np-TFCs show a decrease in the water flux and an enhancement in salt rejection when compared with the unmodified TFC. The most interesting feature of Figure 2 is that these performance

dx.doi.org/10.1021/la403718x | Langmuir 2014, 30, 611−616

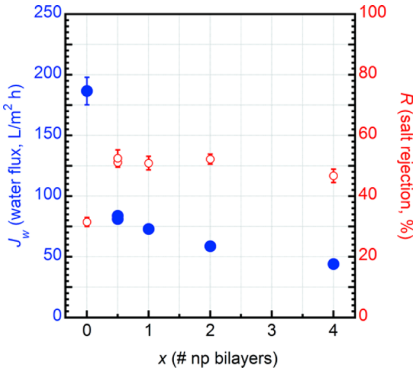

Figure 2. Water flux (closed symbols) and salt rejection (open symbols) performance results of the TFC and np-TFC membranes as a function of np bilayer. The error bars represent one standard deviation of the data, which is taken as the uncertainty of the measurement.

changes are observed even with only a half bilayer of nanoparticles. Specifically, a layer of either positively or negatively charged nanoparticles affects membrane performance by enhancing the salt rejection from ~31% to ~52% while decreasing the water flux from (185 to 80) L m^{-2} h^{-1}, compared with the unmodified TFC. The addition of more nanoparticle bilayers leads to a further decline in water flux but the salt rejection remains relatively unchanged across the various np-TFCs. This trend is in agreement with previously observed effects of material buildup on a membrane surface, such as surface modification or membrane fouling.[3,5,6,8,22] It has been proposed that improvements in salt rejection following the buildup of material on the TFC membrane surface occur due to charge effects within the fouling layer,[3,7] or due to the covering of defects in the membrane active layer.[23,24] Interestingly, although the surface of the virgin NF270 membrane has a negative charge as measured via zeta-potential (Figure S1), the negatively charged nanoparticles do indeed adsorb to the surface of the membrane, which is likely facilitated by nonspecific van der Waals interactions as the anionic nanoparticles are close to their isoelectric point. Furthermore, all of the nanoparticle-modified membranes appear to carry a net negative charge (Figure S1), though the magnitude decreases as the number of bilayers increases. Therefore, charge effects cannot adequately explain the observed flux and rejection behavior.

To explain the changes in performance with nanoparticle deposition, we first recast the performance data in Figure 2 as water and salt flux (Figure 3a). For water flux, this conversion simply changes the traditional unit of flux measurement into SI units. For the salt flux, this requires the conversion of salt rejection into a measure of flux, which is defined as $J_s = J_w c_{s,3}$,[2] where J_w is the water flux and $c_{s,3}$ is the salt concentration on the permeate side. By describing membrane performance in terms of permselectivity (Figure 3b), defined as the ratio of the water flux to the salt flux, we find that the addition of nanoparticles improves the permselectivity of the TFC by over 45% (0.86 to 1.26) at maximum enhancement. Comparing permselectivity with the water flux (Figure 3b), we observe that permselectivity is inversely related to water flux, which is a phenomena referred as performance trade-off and is commonly observed in water purification membranes.[25] The interesting aspect is that previous observations of this performance trade-

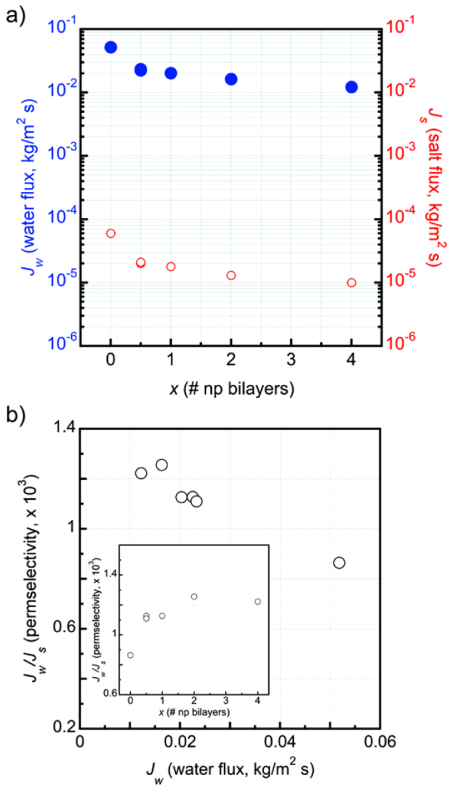

Figure 3. (a) Water (filled symbols) and salt (open symbols) flux of the TFC and np-TFC membranes as a function of np bilayer. The error bars, which are smaller than the symbols, represent one standard deviation of the data, which is taken as the uncertainty of the measurement. (b) Performance trade-off plot comparing permselectivity versus water flux. The inset plot shows the enhancement in permselectivity as a function of np bilayer.

off response required changes in the intrinsic properties of the selective layer, i.e. synthesis of new selective layers with different monomer chemistries.[25] Alternatively, these results demonstrate that the permselectivity of commercial desalination membranes can be enhanced simply via LbL assembly of nanoparticles onto the membrane surface.

Next, we apply the solution-diffusion (SD) model to understand these results. The SD model[26,27] was developed to describe transport through the dense selective layer via the solution diffusion mechanism — transport is a two stage process that first involves partitioning of the permeate into the polymer membrane followed by diffusion of the permeate through the membrane due to an applied pressure.[25] According to the SD model, the water flux of the unmodified TFC ($J_w(0)$) is

$$J_w(0) = A_{nf}(p_2 - p_3 - \Delta\pi) \quad (3)$$

where A_{nf} is the effective water permeance of the TFC, $A_{nf} = P_{nf} m_w / h_{nf} RT$, which is related to the intrinsic and extrinsic properties of the active layer. Here, P_{nf} is the water permeability of the active layer, m_w is the molecular mass of water, h_{nf} is the thickness of the active layer, R is the molar gas constant and T is temperature. Thus, eq 3 suggests that the active layer determines the water permeation rate. For water to permeate through the active layer, the applied pressure difference (Δp) must exceed the osmotic pressure ($\Delta\pi$) of the salt solution, i.e.,

dx.doi.org/10.1021/la403718x | Langmuir 2014, 30, 611−616

to cause the salt and water to "demix". This applied pressure difference is defined by the pressure on the feed side directly at the active layer surface (p_2) minus the pressure on the permeate side (p_3; Figure 4a); the greater this pressure difference, the larger the water flux.

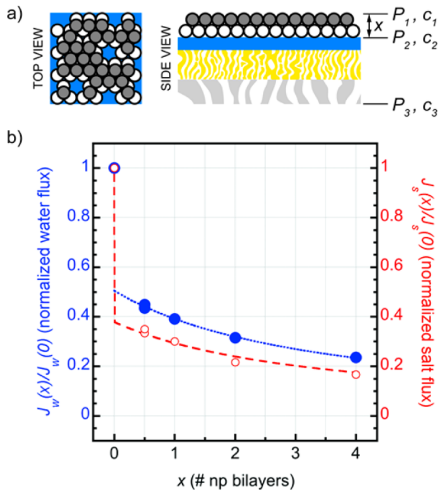

Figure 4. (a) Top and side schematic of the np-TFC. (b) Normalized water (closed symbols) and salt (open symbols) flux of the np-TFC membranes as a function of the number of np bilayers.

The reduction in water flux observed for the np-TFCs can be explained based on this change in pressure difference. From the electron micrographs (Figure 1b), we can consider the nanoparticle layer as a closed-packed assembly of rigid particles where permeation can only occur through the interstitial void spaces between the nanoparticles. This leads to an increase in overall hydraulic resistance, which is equivalent to a decrease in the pressure p_2. To quantify this pressure decrease, we apply the pore flow model to describe the water flux ($J_{w,np}$) through the nanoparticle layer

$$J_{w,np} = A_{np}(p_1 - p_2) \tag{4}$$

where p_1 is the pressure of the feed side directly at the nanoparticle surface (Figure 4a). The water permeability coefficient of the nanoparticle layer is defined as[2]

$$A_{np} = \frac{\varepsilon_{np}}{8\eta_w}\frac{r_{np}^2}{h_{np}} \approx \frac{\varepsilon_{np} r_{np}^2}{8\eta_w}\frac{1}{4r_{np}x} \tag{5}$$

where ε_{np}, r_{np}, and η_w are the porosity, nanoparticle radius, and viscosity of water, respectively. For the purposes of simplifying the analysis, the total thickness of the nanoparticle bilayer is approximated as twice the nanoparticle diameter and the number of bilayers, x, which is defined as $h_{np} \approx 4r_{np}x$.

Mass conservation of water flux at the nanoparticle-TFC interface, i.e., $J_{w,np} = J_w(0)$, yields the expression describing the decrease in pressure at the active layer surface due to presence of the nanoparticle layer, $p_2 = (A_{np}p_1 + A_{nf}\Delta\pi)/(A_{np} + A_{nf})$. In this derivation, we have neglected the p_3 term, as the pressure on the permeate side of the membrane in a dead-end geometry is atmospheric ($p_3 = 0$). Substituting this expression into eq 3 and recognizing the pressure difference for the np-TFC is now $\Delta p = p_1 - p_3 = p_1$, we obtain the following hydraulic resistance-in-series model that describes the water flux of the np-TFC ($J_w(x)$)

$$J_w(x) = \frac{A_{np}A_{nf}}{A_{np} + A_{nf}}(\Delta p - \Delta\pi) \tag{6}$$

This expression implies that the total hydraulic resistance will always increase due to the presence of the nanoparticle layer. In relation to the performance, the water flux is predicted to decrease with increasing nanoparticle layer thickness because the water permeability of the nanoparticle layer scales inversely with the bilayer thickness. Additionally, the nanoparticles reduce the surface area of the TFC (Figure 1b) because water can only flow around these rigid nonporous particles, which eq 6 does not account for. We correct for this reduction in membrane area of the np-TFC ($=a^2(x)$) relative to that of the TFC ($=a^2(0)$) by the 2-dimensional packing fraction of the nanoparticles (ϕ_{np})

$$\frac{\pi(a^2(x))}{\pi(a^2(0))} = (1 - \phi_{np})(1 - \phi_{def}) \tag{7}$$

where ϕ_{def} is the fraction of defects present due to imperfect packing of the nanoparticles, which for the purposes of simplification, we have assumed $\phi_{def} = 0$. A normalized water flux expression is used to compare the np-TFC ($J_w(x)$) with TFC ($J_w(0)$; Figure 4). Combining eqs 3, 6, and 7, we obtain the normalized water flux relationship

$$\frac{J_w(x)}{J_w(0)} = \frac{1 - \phi_{np}}{1 + \frac{A_{nf}}{A_{np}}} \approx \frac{1 - \phi_{np}}{1 + \frac{A_{nf}}{A_{np,(x=1)}}x} \tag{8}$$

where $A_{np,(x=1)} = (\varepsilon_{np}r_{np}^2/8\eta_w)(1/4r_{np})$ defines the water permeability coefficient for a single bilayer of nanoparticles. Hence, eq 8 suggests that the relative change in water flux due the nanoparticle bilayer is determined by (1) the area density of nanoparticles (ϕ_{np}) and (2) the ratio of the water permeability coefficients (A_{nf}/A_{np}). Specifically, increasing the number of nanoparticle bilayers (x) will progressively decrease the normalized water flux for a given np-TFC system since A_{nf}, $A_{np,(x=1)}$ and ϕ_{np} are considered to be constants.

Although the addition of the nanoparticle bilayer leads to a decline in water flux, a positive effect of this surface modification is that it also reduces the salt flux. The expressions of the salt flux for the TFC and np-TFC are related to the respective water fluxes by the following:

$$J_s(0) = J_w(0)c_{s,3}(0) \tag{9}$$

$$J_s(x) = J_w(x)c_{s,3}(x) \tag{10}$$

where $c_{s,3}(0)$ and $c_{s,3}(x)$ are the salt concentrations on the permeate side of the TFC and np-TFC, respectively (Figure 4). A normalized salt flux expression similar to that of the water flux can be developed by combining eqs 9 and 10.

$$\frac{J_s(x)}{J_s(0)} = \frac{J_w(x)}{J_w(0)}\frac{c_{s,3}(x)}{c_{s,3}(0)} \tag{11}$$

Substituting eq 8 into 11 leads to the normalized salt flux expression that shows its dependence to the properties of the nanoparticle layer.

dx.doi.org/10.1021/la403718x | Langmuir 2014, 30, 611−616

$$\frac{J_s(x)}{J_s(0)} \approx \frac{1-\phi_{np}}{1+\frac{A_{nf}}{A_{np,(x=1)}}x}\frac{c_{s,3}(x)}{c_{s,3}(0)} \quad (12)$$

Similar to the normalized water flux expression, the increase in nanoparticle bilayer thickness will lead to a proportional decrease in salt flux for a given np-TFC system as well. The distinction between the two is that the normalized salt flux expression depends also on the salt concentration on the permeate side of the TFC and np-TFC membranes. Importantly, the addition of the nanoparticles does not alter the intrinsic salt rejection ability of the TFC. The presence of the nanoparticle layer alters the salt rejection property in two ways as indicated by eq 11. First, the nanoparticle layer imparts an additional hydraulic resistance, which leads to a reduction in water flux ($J_w(x)/J_w(0)$) and the associated decrease in salt flux since the two permeation events are linked. Second, the presence of the porous nanoparticle layer generates an interface away from the TFC surface that allows for salt accumulation. This accumulation reduces the overall salt concentration (c_2) of the solution at the surface of the TFC ($c_{s,3}(x)/c_{s,3}(0)$), which leads to a lower driving force for salt flux through the TFC membrane because the salt concentration gradient across the TFC is now reduced.

The observed effects of the nanoparticle bilayer thickness on the water and salt fluxes are observed experimentally and confirmed by the empirical fit of eqs 8 and 12 to the normalized water and salt flux results (Figure 4b). Based on these fits, $\phi_{np} \approx 0.50$, $A_{nf} \approx 3.25 \times 10^{-8}$ s/m, $A_{np,(x=1)} \approx 1.12 \times 10^{-7}$ s/m, and $c_{s,3}(x)/c_{s,3}(0) \approx 0.75$ corresponding to the permeability coefficient of the selective layer, the permeability coefficient of a single nanoparticle bilayer and ratio in salt concentration on the permeate side for the np-TFC versus the TFC, respectively. The nanoparticle packing fraction is estimated from the electron micrographs (Figure 1b) by measuring the projected area fraction of the nanoparticles that occupy the membrane area. The ratio $A_{nf}/A_{np,(x=1)} \approx 0.30$ implies that the water permeability of the nanoparticle layer is more than three times greater than the selective layer, which is consistent with the physical picture that the selective layer is dense while the nanoparticle bilayer is porous, consisting of interstitial voids between the nanoparticles. Since the ratio $c_{s,3}(x)/c_{s,3}(0) < 1$ and the intrinsic salt rejection ability of the TFC has not been modified, our results strongly suggest that simple deposition of a nanoparticle layer can enhance the overall salt rejection ability of an existing water desalination membrane.

4. CONCLUSION

We showed that nanoparticle layer-by-layer assembly is an effective means to augment the performance of a commercial TFC nanofiltration membrane. We concluded that the nanoparticles act to diminish, via additional hydraulic resistance, the feed pressure at the surface of the TFC, which in turn decreases the water flux across the TFC membrane. Conversely, the addition of nanoparticle layers served to decrease the salt flux across the TFC membrane, since salt passage is related to some degree on the water flux. Areas for future work include studying the effect of applied pressure, exploring the effect of pH during nanoparticle assembly, and varying nanoparticle size and packing density. Additionally, a cross-flow geometry may impose additional stresses to the nanoparticle layer, thus investigating the mechanical robustness of the nanoparticle-modified membranes is warranted, particularly under shear. Lastly, while this work focused solely on silica nanoparticles, judicious choice of nanoparticles, such as titanium dioxide or silver nanoparticles, may also add to synergistic functions such as self-cleaning or antimicrobial properties to the membrane surface.

■ ASSOCIATED CONTENT

Supporting Information

Zeta potential measurements of np-TFC membranes. This material is available free of charge via the Internet at http://pubs.acs.org.

■ AUTHOR INFORMATION

Corresponding Authors

*E-mail: daeyeon@seas.upenn.edu.
*E-mail: chris.stafford@nist.gov.

Author Contributions

The manuscript was written through contributions of all authors. All authors have given approval to the final version of the manuscript.

Funding

D.L., W.D.M., and Y.R.H. were supported by NSF CAREER Award (DMR-1055594). We also acknowledge the Laboratory for Research on the Structure of Matter at the University of Pennsylvania (MRSEC NSF DMR11-20901) for instrument support. J.-H.L. acknowledges the support by the KIST institutional program (Project No. 2.E23900).

Notes

The authors declare no competing financial interest.

■ REFERENCES

(1) Shannon, M. A.; Bohn, P. W.; Elimelech, M.; Georgiadis, J. G.; Marinas, B. J.; Mayes, A. M. Science and technology for water purification in the coming decades. *Nature* **2008**, *452*, 301−310.

(2) Baker, R. *Membrane Technology and Applications*; John Wiley & Sons: New York, 2004.

(3) Yu, S.; Lü, Z.; Chen, Z.; Liu, X.; Liu, M.; Gao, C. Surface modification of thin-film composite polyamide reverse osmosis membranes by coating N-isopropylacrylamide-co-acrylic acid copolymers for improved membrane properties. *J. Membr. Sci.* **2011**, *371*, 293−306.

(4) Wei, X.; Wang, Z.; Chen, J.; Wang, J.; Wang, S. A novel method of surface modification on thin-film-composite reverse osmosis membrane by grafting hydantoin derivative. *J. Membr. Sci.* **2010**, *346*, 152−162.

(5) Shin, D. H.; Kim, N.; Lee, Y. T. Modification to the polyamide TFC RO membranes for improvement of chlorine-resistance. *J. Membr. Sci.* **2011**, *376*, 302−311.

(6) Louie, J. S.; Pinnau, I.; Ciobanu, I.; Ishida, K. P.; Ng, A.; Reinhard, M. Effects of polyether−polyamide block copolymer coating on performance and fouling of reverse osmosis membranes. *J. Membr. Sci.* **2006**, *280*, 762−770.

(7) Tang, C. Y.; Kwon, Y.-N.; Leckie, J. O. Fouling of reverse osmosis and nanofiltration membranes by humic acid—Effects of solution composition and hydrodynamic conditions. *J. Membr. Sci.* **2007**, *290*, 86−94.

(8) Van Wagner, E. M.; Sagle, A. C.; Sharma, M. M.; La, Y.-H.; Freeman, B. D. Surface modification of commercial polyamide desalination membranes using poly(ethylene glycol) diglycidyl ether to enhance membrane fouling resistance. *J. Membr. Sci.* **2011**, *367*, 273−287.

(9) Azari, S.; Zou, L. Using zwitterionic amino acid l-DOPA to modify the surface of thin film composite polyamide reverse osmosis membranes to increase their fouling resistance. *J. Membr. Sci.* **2012**, *401−402*, 68−75.

(10) Johnson, P. M.; Yoon, J.; Kelly, J. Y.; Howarter, J. A.; Stafford, C. M. Molecular layer-by-layer deposition of highly crosslinked polyamide films. *J. Polym. Sci., Part B: Polym. Phys.* **2012**, *50*, 168−173.
(11) Steiner, Z.; Miao, J.; Kasher, R. Development of an oligoamide coating as a surface mimetic for aromatic polyamide films used in reverse osmosis membranes. *Chem. Commun.* **2011**, *47*, 2384−2386.
(12) Chan, E. P.; Lee, J.-H.; Chung, J. Y.; Stafford, C. M. An automated spin-assisted approach for molecular layer-by-layer assembly of crosslinked polymer thin films. *Rev. Sci. Instrum.* **2012**, *83*, 114102−114102−6.
(13) Gu, J.-E.; Lee, S.; Stafford, C. M.; Lee, J. S.; Choi, W.; Kim, B.-Y.; Baek, K.-Y.; Chan, E. P.; Chung, J. Y.; Bang, J.; et al. Molecular Layer-by-Layer Assembled Thin-Film Composite Membranes for Water Desalination. *Adv. Mater.* **2013**, *25*, 4778−4782.
(14) Shiratori, S. S.; Rubner, M. F. pH-Dependent Thickness Behavior of Sequentially Adsorbed Layers of Weak Polyelectrolytes. *Macromolecules* **2000**, *33*, 4213−4219.
(15) Stanton, B. W.; Harris, J. J.; Miller, M. D.; Bruening, M. L. Ultrathin, Multilayered Polyelectrolyte Films as Nanofiltration Membranes. *Langmuir* **2003**, *19*, 7038−7042.
(16) Saren, Q.; Qiu, C. Q.; Tang, C. Y. Synthesis and Characterization of Novel Forward Osmosis Membranes based on Layer-by-Layer Assembly. *Environ. Sci. Technol.* **2011**, *45*, 5201−5208.
(17) Iler, R. K. Multilayers of colloidal particles. *J. Colloid Interface Sci.* **1966**, *21*, 569−594.
(18) Lee, D.; Rubner, M. F.; Cohen, R. E. All-Nanoparticle Thin-Film Coatings. *Nano Lett.* **2006**, *6*, 2305−2312.
(19) Lee, D.; Omolade, D.; Cohen, R. E.; Rubner, M. F. pH-Dependent Structure and Properties of TiO2/SiO2 Nanoparticle Multilayer Thin Films. *Chem. Mater.* **2007**, *19*, 1427−1433.
(20) Lee, D.; Gemici, Z.; Rubner, M. F.; Cohen, R. E. Multilayers of Oppositely Charged SiO2 Nanoparticles: Effect of Surface Charge on Multilayer Assembly. *Langmuir* **2007**, *23*, 8833−8837.
(21) Dafinone, M. I.; Feng, G.; Brugarolas, T.; Tettey, K. E.; Lee, D. Mechanical Reinforcement of Nanoparticle Thin Films Using Atomic Layer Deposition. *ACS Nano* **2011**, *5*, 5078−5087.
(22) Sagle, A. C.; Van Wagner, E. M.; Ju, H.; McCloskey, B. D.; Freeman, B. D.; Sharma, M. M. PEG-coated reverse osmosis membranes: Desalination properties and fouling resistance. *J. Membr. Sci.* **2009**, *340*, 92−108.
(23) Polyakov, Y. S.; Zydney, A. L. Ultrafiltration membrane performance: Effects of pore blockage/constriction. *J. Membr. Sci.* **2013**, *434*, 106−120.
(24) Tu, K. L.; Chivas, A. R.; Nghiem, L. D. Effects of membrane fouling and scaling on boron rejection by nanofiltration and reverse osmosis membranes. *Desalination* **2011**, *279*, 269−277.
(25) Geise, G. M.; Park, H. B.; Sagle, A. C.; Freeman, B. D.; McGrath, J. E. Water permeability and water/salt selectivity tradeoff in polymers for desalination. *J. Membr. Sci.* **2011**, *369*, 130−138.
(26) Wijmans, J. G.; Baker, R. W. The solution-diffusion model: a review. *J. Membr. Sci.* **1995**, *107*, 1−21.
(27) Paul, D. R. Reformulation of the solution-diffusion theory of reverse osmosis. *J. Membr. Sci.* **2004**, *241*, 371−386.